Equal-intensity waves in non-Hermitian media

I. Komis,[1] S. Sardelis,[2] Z. H. Musslimani,[2] and K. G. Makris[1,3]

[1]*ITCP-Physics Department, University of Crete, Heraklion 71003, Greece*

[2]*Department of Mathematics, Florida State University, Tallahassee, Florida 32306-4510, USA*

[3]*Institute of Electronic Structure and Laser (IESL), FORTH, 71110 Heraklion, Greece*

(Received 17 August 2019; revised 27 May 2020; accepted 28 May 2020; published 3 September 2020)

A novel type of waves is examined in the context of non-Hermitian photonics. We can identify a class of complex guided structures that support localized paraxial solutions whose intensity distribution is exactly the same as the intensity of a corresponding solution in homogeneous media (free or bulk space). In other words, intensity-wise the two solutions are identical and their phase is different by a factor $\exp[i\theta(x, y)]$. The non-Hermitian potential is determined by the phase θ, as well as the amplitude and phase of the bulk space solution that contributes to the imaginary and real part of the potential, respectively. That way we can connect the plane waves and Gaussian beams of free space to constant-intensity waves and what we call the equal-intensity waves (EI waves) in non-Hermitian media. Such a relation allows us to study three different physical problems: Propagating EI waves inside random media, interface lattice solitons, and moving solitons in photonic waveguide structures with free-space characteristics. The relation of EI waves to unidirectional invisibility and Bohmian photonics is also examined.

DOI: 10.1103/PhysRevE.102.032203

I. INTRODUCTION

Non-Hermitian Hamiltonians in classical and quantum physics [1] describe the dynamics of open systems under the influence of dissipation and/or amplification. Among their unique characteristics are the existence of non-Hermitian degeneracies [2] or exceptional points [3], where two or more eigenvalues and eigenvectors coalesce for a particular value of a system's parameter [4,5]. Nonorthogonal modes, excess noise, a complex spectrum, and nonconservation of power are some of their mathematical features. One special class of non-Hermitian Hamiltonians are those that respect parity-time ($\mathcal{PT}$) symmetry [6]. In a number of studies it has been shown that such a class may exhibit entirely real or partially complex eigenvalue spectra with conjugate pairs of eigenvalues [7,8].

Over the past ten years, considerable effort has been devoted to the realization of these counterintuitive ideas in the field of optical physics. Indeed, based on the theoretical [9–11] and experimental studies [12,13] related to waveguided photonic structures, these mathematical notions led to the new area of $\mathcal{PT}$-symmetric optics. In this respect, loss can be considered as an asset in optics as opposed to being a foe, provided it can be judiciously used to realize this new class of $\mathcal{PT}$-symmetric optical systems. The plethora of novel concepts and experimental applications that have been recently reported, such as coherent perfect absorbers, unidirectional invisibility, broadband wireless power transfer, single-mode nanolasers, nonreciprocal microresonators, ultrasensitive sensors based on a higher order of exceptional points, $\mathcal{PT}$-symmetric phonon lasers, and solitons in $\mathcal{PT}$-lattices, is really surprising [14–24]. The degree of intense research activity in this new field of non-Hermitian photonics is reflected in the large number of recent review articles and special issues devoted to this area [25–32].

Within the context of non-Hermitian photonics, the concept of "constant-intensity waves"(CI waves) was recently introduced [33]. Such novel waves are exact solutions of the linear and nonlinear wave equations (paraxial and wave scattering regime), and they provide an ideal way for studying modulation instability in inhomogeneous structures [33–35], and perfect transmission in strongly scattering disordered media [36]. CI waves exist for the general class of non-Hermitian Wadati potentials of the form $V(x) = W^2(x) - i\frac{dW}{dx}$ for every real smooth function $W(x)$. This function determines the real and imaginary parts of the complex potential, and it is also directly related to the phase of the CI waves as well as the Poynting vector power flow [33,36]. These waves were experimentally realized in the acoustics regime [37], where engineering the gain and loss distributions across a one-dimensional random medium leads to perfect constant pressure waves that overcome the Anderson localization effects. Two-dimensional generalization of CI waves was also studied in scattering systems [38]. Using such schemes, not only can the scattering amplitudes be engineered to render an object unidirectionally invisible [39,40], but also the near-field features can be effectively suppressed through constant-intensity waves in inhomogeneous scattering landscapes [39,40]—a feature that is inaccessible in Hermitian disordered environments [41–45].

In this paper, we examine generalizations of CI waves. Since CI waves are the analogs of free-space plane waves inside non-Hermitian structures, a natural question one may ask is what is the corresponding analog of a Gaussian beam? Is there a systematic way to associate the homogeneous space solutions to confined solutions of inhomogeneous wave equations for a non-Hermitian system? More specifically, we investigate the conditions under which one can obtain a relation between the solutions of the paraxial wave equation (bulk media) and the inhomogeneous wave equation (non-Hermitian media). By applying such a transformation, is possible to connect the intensities of the two solutions provided that the corresponding potential in non-Hermitian. Apart from a phase factor, the two different solutions have equal intensities in any point of space. This phase factor is directly related to the real and imaginary parts of the complex potential. By applying such a concept, we were able to derive new families of paraxial beam solutions in z-dependent complex potentials, as well as classes of analytical interface soliton solutions for both one- and two-dimensional structures. The paper is organized as follows: In Secs. II and III the transformation between linear wave equations is examined in detail by providing pertinent examples. In Secs. IV, V, VI, and VII the extension in the nonlinear domain is systematically investigated.

II. EQUAL-INTENSITY BEAMS IN LINEAR MEDIA

Our starting point is the paraxial equation of diffraction in an inhomogeneous waveguide system, which in normalized units is given by

$$iU_z + \nabla_\perp^2 U + V(x, y, z)U = 0, \quad (1)$$

where $\nabla_\perp^2 \equiv \frac{\partial^2}{\partial x^2} + \frac{\partial^2}{\partial y^2}$ denotes the transverse Laplacian in the two spatial transverse coordinates, and $U_z = \frac{\partial U}{\partial z}$ is the evolution term of the field's envelope along the propagation direction z. The physical photonic structure is that of an optical z-dependent potential $V(x, y, z)$ [10,30]. On the other hand, the propagation of waves in free or bulk space is described by the paraxial equation of diffraction. Free or bulk media are mathematically equivalent here, and the diffraction of waves is described by the same normalized equation (thus these two terminologies will be used equivalently), which is

$$i\phi_z + \nabla_\perp^2 \phi = 0. \quad (2)$$

The question that we are dealing with in this paper is if we can relate these two different problems (in terms of field intensities) by allowing the optical potential $V(x, y, z)$ to be complex. In other words, we require the intensities of the two different solutions to be equal:

$$|\phi(x, y, z)|^2 = |U(x, y, z)|^2, \quad (3)$$

which leads us naturally to the following relation:

$$U(x, y, z) = \phi(x, y, z)\exp[i\theta(x, y)]. \quad (4)$$

The only way we can connect the intensities of the two equations for any arbitrary phase factor $\theta(x, y)$ is by allowing the potential $V(x, y, z)$ to be complex. By expressing the homogeneous space solution ϕ in the form $\phi(x, y, z) = \phi_A(x, y, z)\exp[i\phi_P(x, y, z)]$, where $\phi_A(x, y, z)$ and $\phi_P(x, y, z)$ are the real functions of the amplitude and phase of the field, respectively, we can write the corresponding non-Hermitian potential in the following general form (where the gradient operator ∇ always refers to two spatial dimensions, in all the remaining sections):

$$V = \nabla\theta \cdot \nabla[\theta + 2\phi_P] - i[\nabla^2\theta + 2\nabla\theta \cdot \nabla \ln\phi_A]. \quad (5)$$

As we can see from the preceding equation, since the field's envelope function $\phi(x, y, z)$ is complex, its amplitude ϕ_A affects the imaginary part of the optical potential, whereas the phase ϕ_P contributes to the real part. At this point, let us better understand the features of this relationship, which lead us to a novel class of non $\mathcal{PT}$-symmetric complex potentials. First of all, this is a nonlinear transformation in the sense of Cole-Hopf transform between the Burgers equation and the heat equation. Moreover, since any pair of ϕ, U corresponds to a different potential $V(x, y, z)$, a superposition of two different ϕ's will not lead to a superposition of the complex potentials. Secondly, the function $\theta(x, y)$ does not depend on the solution ϕ. This means that we can choose any function θ for the same solution ϕ. Furthermore, by using such a transformation, we can relate any known solution of the free space, that does not have zeros at different locations from its derivative, to an infinite number of z-dependent complex potentials that contain gain and loss and are determined by $\theta(x, y)$.

Another important aspect we would like to examine is the relation of the CI waves [33] to the aforementioned equal-intensity (EI) waves. Let us choose the most fundamental solution of the free-space paraxial equation of diffraction, Eq. (2), which is the plane wave:

$$\phi(x, y, z) = e^{i(\beta z - k_x x - k_y y)} \quad (6)$$

with a parabolic dispersion relation $\beta = k_x^2 + k_y^2 = \vec{k}^2$ between the propagation constant β and the transverse wave vector $\vec{k}$. Obviously it is true that $\nabla[2\ln\phi_A] = 0$ and $\nabla\phi_P = -\vec{k}$. Therefore, by substituting into the preceding equation Eq. (5), we get the following potential:

$$V(x, y, z) = \nabla\theta \cdot \nabla\theta - 2\vec{k} \cdot \nabla\theta - i\nabla^2\theta, \quad (7)$$

which for $\vec{k} = 0$ (propagation parallel to the z-direction) leads us to the non-Hermitian Wadati potential $V(x, y) = \nabla\theta \cdot \nabla\theta - i\nabla^2\theta$ that support CI waves of the form $U = \exp[i\theta(x, y)]$ [33].

At this point, we have to mention the difference between our work and the recently introduced two-dimensional potentials of Bohmian photonics [38]. Apart from the fact that such waves refer to the Helmholtz scattering wave equation (two-dimensional) and not to the paraxial equation of diffraction ($2 + 1$ dimensions), the function ϕ is not some arbitrary design intensity pattern, but it satisfies the free-space wave equation. This allows us to connect two different wave equations and use the bulk space solutions to construct non-Hermitian structures with free-space characteristics.

III. EQUAL-INTENSITY GAUSSIAN BEAMS

An initial example of a non-Hermitian structure that supports solutions with free-space characteristics can be obtained if we connect the paraxial Gaussian beam of free space to a corresponding EI wave. The Gaussian beam analytical solution of Eq. (2) (in one spatial dimension) is given in normalized units by the following expression:

$$\phi(x, z) = \left(\frac{2}{\pi w^2}\right)^{1/4} \exp\left(-\frac{x^2}{w^2} + i\frac{x^2}{2R} - i\frac{\varphi_0}{2}\right), \quad (8)$$

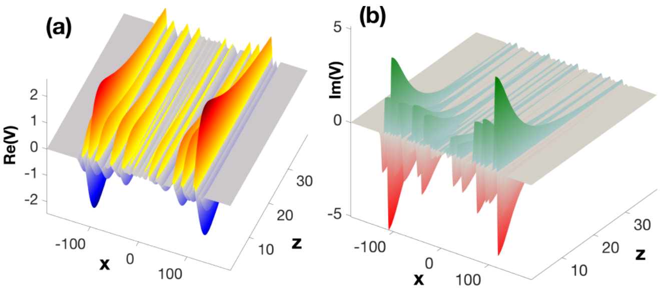

FIG. 1. A non-Hermitian z-dependent random potential that supports an EI wave with equal intensity to that of the free-space Gaussian beam. In (a),(b) the real and imaginary parts of the $V(x, z)$ are depicted, respectively.

where

$$R(z) = 2z + \frac{1}{z}\frac{w_0^4}{8}, \tag{9}$$

$$w(z) = w_0\sqrt{1 + \left(\frac{4z}{w_0^2}\right)^2}, \tag{10}$$

$$\tan \varphi_0 = \frac{4z}{w_0^2}. \tag{11}$$

R, w, φ_0 are the beam's curvature, the beam's waist, and the Gouy phase shift, respectively. The one-dimensional analog of Eq. (5) is

$$V(x, z) = \left[\theta_x^2 + 2\theta_x \phi_{Px}\right] - i[\theta_{xx} + 2\theta_x(\ln\phi_A)_x]. \tag{12}$$

By substituting Eq. (8) into Eq. (12), we obtain the following family of complex potentials:

$$V(x, z) = \theta_x^2 + 2\theta_x \frac{x}{R(z)} + i\left(4\theta_x \frac{x}{w^2(z)} - \theta_{xx}\right). \tag{13}$$

Notice that the above potential depends on both x and z coordinates and describes a general family of complex potentials, which are not $\mathcal{PT}$-symmetric in general, for any smooth function $\theta(x)$. For example, the function $\theta(x) = \frac{x^2}{2}$ leads to a parabolic potential with z-dependent gain and loss refractive index distributions, which supports a beam solution with an intensity profile exactly the same as that of free space.

To highlight the nontrivial aspects of the EI waves and their physical implications, we will relate the free-space evolution of a Gaussian beam to that inside a disordered medium in order to achieve undistorted propagation against transverse disorder. For this reason, we choose the $\theta(x)$-function to be a random superposition of N Gaussian functions with random widths w_n and positions c_n. In particular, we have

$$\theta(x) = \sum_{n=1}^{N} A e^{-(\frac{x-c_n}{w_n})^2}. \tag{14}$$

Substitution of Eq. (14) into Eq. (13) leads to a z-dependent disordered potential, which in the Hermitian limit (when gain and loss are absent) supports localized eigenmodes. The real and imaginary parts of this complex potential as a function of the propagation distance z are presented in Figs. 1(a) and 1(b), respectively. The corresponding diffraction dynamics is depicted in Fig. 2. In fact, we see that when the imaginary part is zero (Hermitian case), then the beam is mostly trapped inside the disordered index variation [Fig. 2(a)] due to Anderson localization in the transverse direction. On the other hand, when we consider the full non-Hermitian potential [Fig. 2(b)], then the wave diffracts exactly as a Gaussian beam in free space. This means that in these two different physical problems, the beam's intensity profiles are identical. In particular, the comparison between the beam's intensity at $z = 40$ in free space (green line) and inside the non-Hermitian potential (dashed black line) is shown in Fig. 2(c).

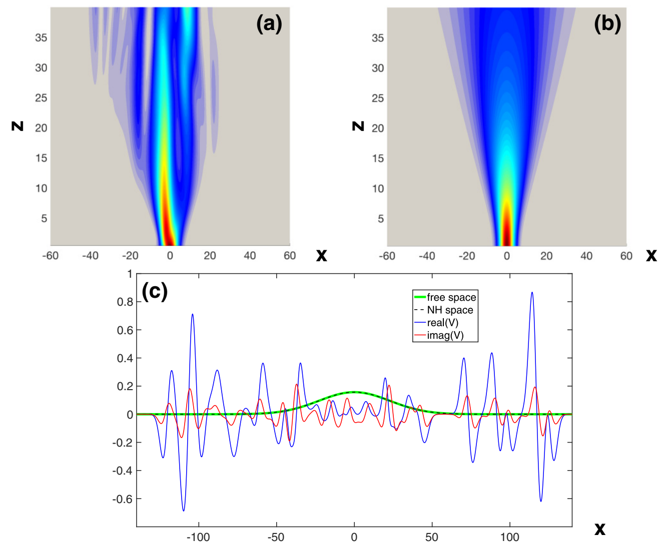

FIG. 2. The intensity of a propagating Gaussian beam in (a) a real random potential, and (b) inside the corresponding non-Hermitian random potential. The absolute value of the diffracted field at $z = 40$ is depicted in (c). In particular, we can see the direct comparison between the $|U|$ inside the non-Hermitian potential (dashed black line) and the corresponding $|\phi|$ of a Gaussian beam (with a width at focus equal to $w_0 = 5$) in free space (green line). The two intensity profiles are identical. Also the real (blue line) and imaginary (red line) parts of the $V(x, 40)$ are shown.

So far we have seen that a plane wave in free space corresponds to a CI wave, and a Gaussian beam corresponds to an EI wave. One may wonder if we can derive other EI waves by considering different known solutions of the free-space equation of diffraction, such as higher-order Gaussian beams, diffraction-free Bessel beams, or accelerating Airy beams. In these cases, the field has zeros in different locations from its derivative, and therefore singularities appear in the potential of Eq. (5).

IV. NONLINEAR EI WAVES

The above ideas that connect a non-Hermitian system with the bulk space can be directly applied to the nonlinear regime in order to construct complex guided structures with free-space-like characteristics. Thus, the wave evolution in a nonlinear Kerr medium is described by the inhomogeneous nonlinear Schrödinger equation (NLSE), which in normalized units reads

$$iU_z + U_{xx} + V(x)U + |U|^2U = 0. \tag{15}$$

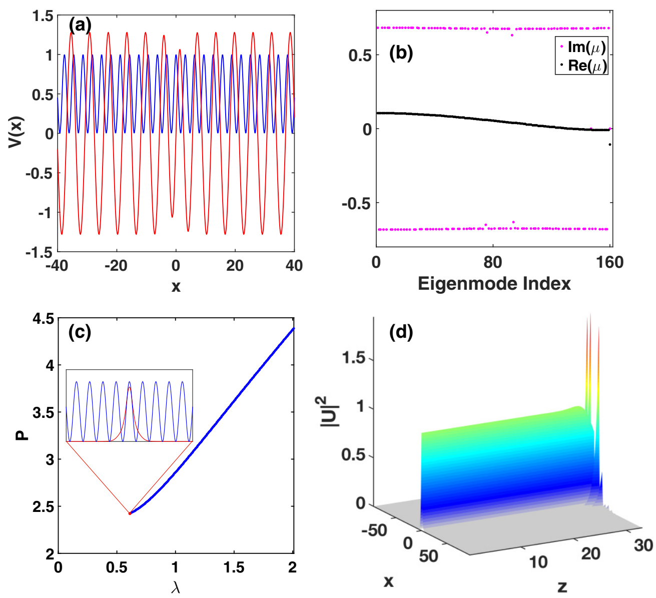

FIG. 3. (a) Real (blue line) and imaginary (red line) parts of the complex potential vs the spatial coordinate x. (b) Real (black color) and imaginary (magenta color) parts of the linear eigenvalue spectrum (μ) vs the eigenmode ($\tilde{u}$) index for 160 lattice cells, of the $\cos^2(x)$, and imposed periodic boundary conditions. (c) Power (P) eigenvalue (λ) diagram of the interface lattice soliton. Here the inset depicts the soliton's intensity (red line) for $P \approx 2.5$. The real part of the lattice is also presented (blue line) for comparison in the inset. (d) Dynamics of soliton for $\lambda = 0.68$. As we can see, the soliton appears to be unstable after $z \sim 33$ under the influence of random perturbations.

Stationary soliton solutions have the following form:

$$U(x, z) = u(x)\exp(i\lambda z), \tag{16}$$

where $u(x)$ is the complex valued field profile and λ is the nonlinear propagation constant. By substituting this last ansatz into Eq. (15), we get the following nonlinear eigenvalue problem:

$$u_{xx} + V(x)u + |u|^2 u = \lambda u. \tag{17}$$

The above eigenvalue problem is a nonlinear one since the nonlinear eigenvalue λ and the soliton profile $u(x)$ are nontrivially related and there is no guarantee that a solution even exists or how many solutions we have in the first place. Rigorously speaking, $u = u(x, \lambda)$, and we use iteration renormalization techniques (see the next section) to numerically determine the relation between the soliton's power $P = P(\lambda) \equiv \int_{-\infty}^{+\infty} |u(x, \lambda)|^2 dx$ and the nonlinear propagation constant λ (power-eigenvalue diagram) [46,47]. Before we study the above nonlinear eigenvalue problem, it is always beneficial to understand the underlying linear eigenvalue problem, namely

$$\tilde{u}_{xx} + V(x)\tilde{u} = \mu\tilde{u}, \tag{18}$$

which is obtained by the linear version of Eq. (17) when looking for the eigenmode profiles $U(x, z) = \tilde{u}(x)\exp(i\mu z)$.

We can now relate the solutions of the inhomogeneous NLSE of Eq. (15) to a bulk space NLSE, which is given by

$$i\phi_z + \phi_{xx} + |\phi|^2\phi = 0. \tag{19}$$

The corresponding nonlinear eigenvalue problem is obtained by looking for solutions of the type $\phi(x, z) = \rho(x)\exp(i\lambda z)$, where $\rho(x)$ is a positive real function of x. Therefore, we have

$$\rho_{xx} + \rho^3 = \lambda\rho. \tag{20}$$

The two nonlinear eigenvalue problems of Eqs. (17) and (20) are directly related if one assumes a complex potential. More specifically, by considering a solution of Eq. (17) of the form $u(x) = \rho(x)\exp[i\theta(x)]$, with $\rho(x), \theta(x)$ real functions of position x, one can relate any solution of Eq. (17) to the corresponding bulk problem. For such an assumption to be true, we must allow the potential to be complex, $V(x) = V_R(x) + iV_I(x)$. In fact, it must have the following form: $V(x) = \theta_x^2 - i[\theta_{xx} + 2\theta_x(\ln\rho)_x]$. Notice that the real part of the potential does not depend on the solution profile ρ but only on θ. This is expected, since in this case $\phi_P(x) = 0$ and $\phi_A(x) = \rho(x)$. The above analysis is general and it relates two different nonlinear eigenvalue problems, that of the homogeneous and inhomogeneous complex NLSE. Moreover, it allows us to construct non-Hermitian structures that support nonlinear EI waves with bulk space characteristics. Given a stationary solution ρ of the bulk NLSE eigenvalue problem, we can derive a complex potential that supports a nonlinear EI wave with bulk-space-like intensity profiles. The simplest example is that of the fundamental solution of the NLSE, the bright soliton of the form $\rho(x) = A\,\mathrm{sech}(bx)$. For any real-valued function $\theta(x)$, the corresponding complex potential is

$$V(x) = \theta_x^2 - i[\theta_{xx} - 2b\theta_x \tanh(bx)]. \tag{21}$$

We are going to examine in the next section how one can numerically identify the supported nonlinear EI waves of the above potential by direct application of the spectral renormalization method [48]. It is of particular interest to consider $\mathcal{PT}$-symmetric periodic potentials. In other words, we will examine complex potentials that are $\mathcal{PT}$-symmetric provided that their real part is even in x, and the imaginary component (that describes the loss or gain) is odd. In other words, the necessary but not sufficient condition for $\mathcal{PT}$-symmetry, namely $V(x) = V^*(-x)$, must be satisfied [11].

Before we proceed to particular one-dimensional examples, we would like to note that nonlinear EI waves also exist in two spatial dimensions. In particular, let us consider the two-dimensional normalized nonlinear Schrödinger equation with a complex potential:

$$iU_z + U_{xx} + U_{yy} + V(x, y)U + |U|^2 U = 0. \tag{22}$$

The methodology that we follow here is similar to the one we followed for the one-dimensional problems. Hence, by assuming $U(x, y) = u(x, y)e^{i\lambda z}$, where $u(x, y)$ represents the complex soliton field profile and λ is the propagation constant or the soliton's eigenvalue, we get the nonlinear eigenvalue problem $\nabla^2 u + V(x, y)u + |u|^2 u = \lambda u$. By substituting $\phi(x, y, z) = \rho(x, y)e^{(i\lambda z)}$ into the two-dimensional bulk NLSE, $i\phi_z + \nabla^2\phi + |\phi|^2\phi = 0$, we get the nonlinear eigenvalue problem for $\rho(x, y)$, namely $\nabla^2\rho + \rho^3 = \lambda\rho$. Since there are no analytical solutions for the last bulk nonlinear eigenvalue problem, we apply an iterative spectral renormalization method to identify stationary solutions. Based on these solutions, we can (only computationally) determine the corresponding non-Hermitian potential $V(x, y)$, which supports nonlinear EI waves:

$$V(x,y) = \nabla\theta\cdot\nabla\theta - i[\nabla^2\theta + 2\nabla\theta\cdot\nabla\ln\rho]. \quad (23)$$

V. SPECTRAL RENORMALIZATION METHOD

Since we are dealing with nonlinear eigenvalue problems, it is beneficial to briefly present here the spectral renormalization method, which is a self-consistent computational technique for finding stationary soliton solutions of the inhomogeneous nonlinear Schrödinger equation. The spectral renormalization approach was first introduced by Ablowitz and Musslimani [48] to numerically construct a family of localized soliton solutions of the NLSE on bulk or lattice systems. In fact, by using such a method we can numerically compute localized soliton solutions to both one- and two-dimensional NLSEs in non-Hermitian potentials [11]. The method can be applied for any potential (periodic or not) by using finite-difference or spectral derivative schemes.

Here we will work on the spectral domain and use Fourier transforms. These transforms in the spatial domain are defined as follows:

$$\hat{u}(k) = \mathcal{F}[u(x)] = \int_{-\infty}^{\infty} u(x)e^{-ikx}dx, \quad (24)$$

$$u(x) = \mathcal{F}^{-1}[\hat{u}(k)] = \frac{1}{2\pi}\int_{-\infty}^{\infty} \hat{u}(k)e^{ikx}dk. \quad (25)$$

By taking the Fourier transform of Eq. (17), we have

$$-\lambda\hat{u}(k) - k^2\hat{u}(k) + \mathcal{F}[V(x)u(x)] + \mathcal{F}[|u(x)|^2u(x)] = 0, \quad (26)$$

which leads us to the relation

$$\hat{u}(k) = \mathcal{M}[\hat{u}(k)], \quad (27)$$

where $\mathcal{M}$ is defined as

$$\mathcal{M}[\hat{u}(k)] = \frac{\mathcal{F}[V(x)u(x)] + \mathcal{F}[|u(x)|^2u(x)]}{\lambda + k^2}. \quad (28)$$

Equation (26) is an infinite-dimensional fixed-point equation for $\hat{u}(k)$ that will be solved using the spectral renormalization method. At this point, we also note that we are looking for solutions with $\lambda > 0$. On that basis, since we want to construct a condition that limits the amplitude under iteration from either growing without bound or tending to zero, we introduce a new field variable s such that

$$u(x) = rs(x), \quad \hat{u}(k) = r\hat{s}(k), \quad (29)$$

where r is the renormalization constant ($r \neq 0$) to be determined. By iteration, all s_n are given by the following relation:

$$\hat{s}_{n+1} = \mathcal{M}[\hat{s}_n(k), r_n], \quad (30)$$

where $\mathcal{M}[\hat{s}_n(k), r_n]$ is given by the expression

$$\mathcal{M}[\hat{s}_n(k), r_n] = \frac{\mathcal{F}[V(x)s_n(x)] + |r_n|^2\mathcal{F}[|s_n(x)|^2s_n(x)]}{\lambda + k^2}. \quad (31)$$

Now the renormalization constant r_n at every iteration step can be directly determined by Eq. (26). After substituting Eq. (29), multiplying both sides with $\hat{s}_n^*(k)$, and integrating in all k-space, we get the following equation for $|r_n|^2$:

$$\int_{-\infty}^{\infty} |\hat{s}_n(k)|^2dk = \int_{-\infty}^{\infty} \hat{s}_n^*(k)\frac{\mathcal{F}[V(x)s_n(x)]}{\lambda + k^2}dk + |r_n|^2\int_{-\infty}^{\infty} \hat{s}_n^*(k)\frac{\mathcal{F}[|s_n(x)|^2s_n(x)]}{\lambda + k^2}dk. \quad (32)$$

From the preceding equation we can directly determine the renormalization constant r_n, which one can show is a real number (due to the gauge invariance of the inhomogeneous NLSE). Once we know the renormalization constant at every iteration step, we can determine the corresponding solution from Eq. (28). Once the scheme converges and the error between successive solutions tends to zero, the inverse Fourier transform of $\hat{u}(k)$ leads us to the desired stationary soliton solution $u = u(x, \lambda)$. Direct generalization of this method to two spatial dimensions is possible [11].

VI. FREE-SPACE-LIKE LATTICE SOLITONS

In this section, we are going to apply the spectral renormalization method to obtain nonlinear EI waves in guided non-Hermitian structures. For reasons of physical relevance, we choose $\theta(x)$ to be the periodic function $\theta(x) = \sin x$. Then based on Eq. (21) we get the following complex $\mathcal{PT}$-symmetric potential:

$$V(x) = \cos^2 x + i[\sin x + 2b\cos x\tanh(bx)]. \quad (33)$$

First of all, the real part of the potential is indeed a periodic function, whereas the imaginary part describes two different semi-infinite lattices with a defect around $x = 0$. The width of the defect is determined by the parameter b. The real and imaginary parts of this potential are shown in Fig. 3(a), and the corresponding linear eigenvalue spectrum based on Eq. (18) is shown in Fig. 3(b) for the case in which $b = 0.4$. Here we consider a finite number of cells and impose periodic boundary conditions at both ends of the finite lattice. Therefore, the above potential describes physically a refractive index modulation profile that corresponds to a perfectly periodic real potential with an imaginary defect at $x = 0$, which separates two imaginary semi-infinite lattices. This means that we expect to have a surface lattice soliton at the interface ($x = 0$) with a power threshold [46,47]. For $b = 0.4$ this threshold is $P_{\text{th}} \approx 2.5$, as is evident from the power eigenvalue diagram of Fig. 3(c). The lattice soliton, as one can see in the inset of Fig. 3(c), does not have peaks at the center of each waveguide but rather a smooth intensity profile, like the fundamental soliton of NLSE. Furthermore, by applying spectral beam propagation methods, we can examine the nonlinear stability of our soliton solutions. As we can deduce from Fig. 3(d), the interface soliton for $b = 0.4$ appears to be unstable. Since the soliton's stability is not our main focus here, we did not perform linear stability analysis. Our goal is to use the non-Hermitian transformation in order to enhance the wave's transport through complex media.

Two-dimensional non-Hermitian lattices, which support solitons with free-space features, can also be derived based on Eq. (23). More specifically, direct application of the

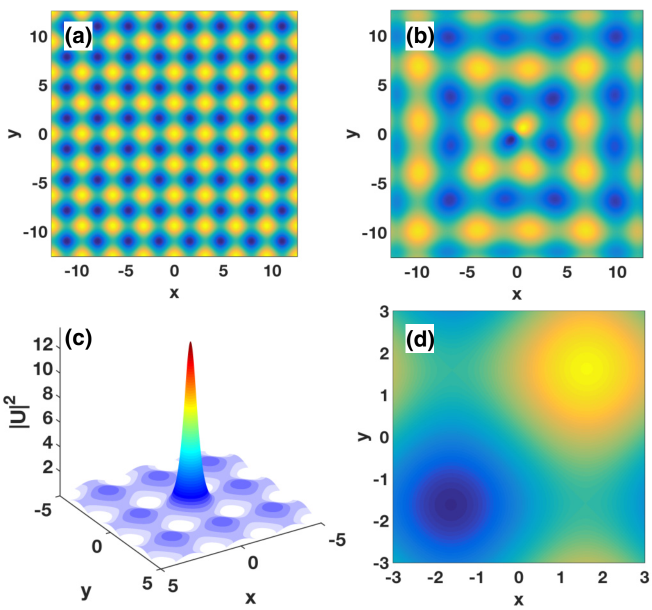

FIG. 4. (a) Real and (b) imaginary part of the two-dimensional non-Hermitian optical lattice. In (c) the lattice soliton's intensity is depicted, and in (d) the corresponding phase distribution is shown (for $\lambda = 3$).

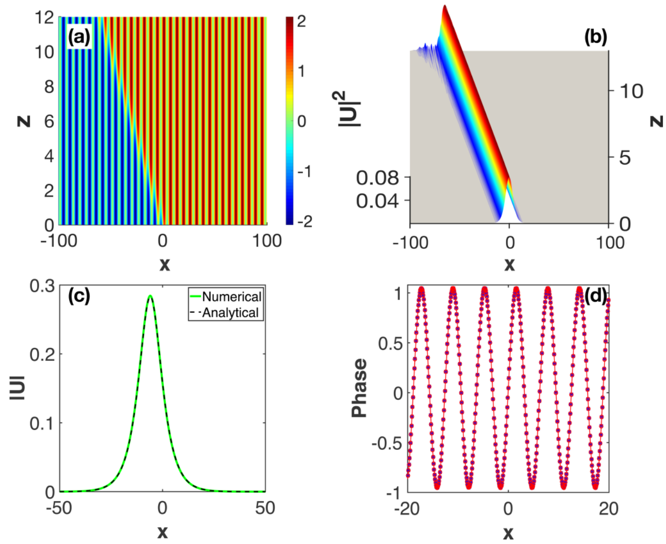

FIG. 5. (a) Imaginary part of the lattice $V(x,z)$ as a function of the propagation distance and (b) the intensity of the moving soliton's evolution across the lattice interface. In the bottom figures we compare the analytically and numerically obtained solutions at a propagation distance of $z = 1.2$. In particular, we compare the numerically and analytically obtained moving soliton solutions for (c) the absolute value of the field, and (d) the phase profile. As we can see, the agreement is perfect.

spectral renormalization method provides the numerical solutions $\rho(x,y)$ for the bulk two-dimensional NLSE, and therefore we can obtain the potential of Eq. (23) only numerically (and not analytically, as in the one-dimensional case). Furthermore, we choose a physically relevant periodic phase $\theta(x,y)$, namely $\theta = \sin x + \sin y$. Our results are shown in Fig. 4. In Figs. 4(a) and 4(b), the real and imaginary parts of the complex potential, based on a $\rho(x,y)$ solution for $\lambda = 2$, are illustrated. In Figs. 4(c) and 4(d), we present the lattice soliton intensity and its phase, respectively. The free-space characteristic of the soliton here is the circular symmetry of its intensity profile despite the fact that there is coupling to several nearest-neighboring lattice sites.

VII. MOVING SOLITONS IN NON-HERMITIAN LATTICES

An interesting problem in the context of nonlinear lattice physics is to examine if moving solitons are possible in a periodic potential [49]. Most of the existing studies are focused on complicated analytical techniques limited by the inherent approximations of a discrete NLSE for Hermitian systems. In this section, we can approach such a problem in a different way based on nonlinear EI waves. By relating the bulk space, where traveling solitons are possible due to translational symmetry, to an appropriate non-Hermitian structure, we can obtain nonlinear EI waves by considering potentials that have suitable gain and loss distributions.

In particular, we require that the field amplitude is z-dependent as well. This means that $U(x,z) = \rho(x,z)e^{i\theta(x)}e^{i\lambda z}$. Thus, the desired potential has the following form:

$$V(x,z) = \theta_x^2 - i[\theta_{xx} + 2\theta_x(\ln\rho)_x + (\ln\rho)_z], \qquad (34)$$

where $\rho(x,z)$ satisfies the equation $\lambda\rho - \rho_{xx} - \rho^3 = 0$. If we assume now a moving soliton solution for ρ, namely $\rho(x,z) = A\,\text{sech}(bx + az)$, we get the following general family of non-Hermitian potentials:

$$V(x,z) = \theta_x^2 - i[\theta_{xx} - (2b\theta_x + a)\tanh(bx + az)]. \qquad (35)$$

Notice that only the imaginary part of the potential depends on z, a fact that is physically expected since the phase of the bulk solution (which contributes to the real part of V) is zero. A particular case of interest, as before, is when the phase factor is periodic, meaning that $\theta(x) = \sin x$. Thus we get the non-Hermitian potential:

$$V = \cos^2 x + i[\sin x + (2b\cos x + a)\tanh(bx + az)], \qquad (36)$$

which supports the nonlinear EI-wave solution $U(x,z) = \sqrt{2}b\,\text{sech}(bx + az)e^{i\sin x}e^{ib^2 z}$. Our results are depicted in Fig. 5 for the parameter values of $a = 1$ and $b = 0.2$. The real part of the potential is a period lattice, whereas the corresponding imaginary part is illustrated in Fig. 5(a). Instead of a periodic lattice, we have two tilted semi-infinite lattices, one with a gain modulation (on the left) and another that is lossy (on the right). The soliton travels [Fig. 5(b)] across this titled interface for several coupling lengths before instabilities destroy its invariant spatial profile. A comparison between the analytically and the computationally obtained solution is shown for $z = 1.2$ in Figs. 5(c) and 5(d) for the amplitude and phase, respectively. What is remarkable is that we can construct a non-Hermitian structure that has no translational symmetry, but nevertheless supports a nonlinear EI wave with bulk space features. In this case, the relevant feature is a traveling soliton in free space.

VIII. DISCUSSION AND CONCLUSIONS

In this paper, we have derived non-Hermitian structures that support solutions with free-space characteristics. In particular, we found that such solutions are different from free-space solutions only by a nonconstant phase given by a parameter function $\theta(x, y)$. This phase directly determines the complex potential that describes the inhomogeneous space. In the context of non-Hermitian photonic systems, we have examined various pertinent examples of guided paraxial structures in linear and nonlinear regimes and also in one and two spatial dimensions. We note here that the CI waves, which are supported by Wadati potentials [50–54], are a limiting case of the general family of solutions we study in this work. We note that there are various analytical methods for constructing analytical solutions in complex potentials [50–56], but we emphasize here that our focus is the underlying physical behavior of the obtained non-Hermitian potentials.

A potential application of our non-Hermitian transformation between two different systems could relate the recently discovered nonlocal integrable NLSE [57] and the non-Hermitian inhomogeneous wave equation. Such an integrable equation has the form $\rho_{xx} + \rho^2(x)\rho^*(-x) = \lambda\rho$, where $\rho(x)$ is now a complex function. By setting $\tilde{u}(x) = \rho(x)\exp[i\theta(x)]$ and demanding $\tilde{u}_{xx} + V(x)\tilde{u} = \lambda\tilde{u}$, we can find after some algebra the corresponding non-Hermitian potential, $V(x) = \theta_x^2 + \rho\rho^*(-x) - 2i\theta_x(ln\rho)_x - i\theta_{xx}$. So far there is no physical system that this integrable nonlocal equation describes. This transformation could provide a systematic way of finding an optical guided structure that under specific conditions supports solutions with the same intensity profiles as the nonlocal integrable NLSE.

In conclusion, we have shown that the complex nature of an optical potential (complex refractive index in photonics) can provide us with an extra degree of freedom of controlling the flow of light inside complex media. This unique class of solutions exists only in non-Hermitian potentials, and we call them equal-intensity waves (EI waves). The phase of these waves affects the real part of the potential, whereas their amplitude affects the imaginary part. By applying this concept, we addressed three different physical problems, namely transport of light in disordered media, nonlinear EI waves at interfaces, and moving lattice solitons, by including the appropriate imaginary part to the refractive index modulation profile. Eliminating the reflections and connecting the wave propagation inside complex media to free space diffraction is also related to transformation optics related ideas in photonics and metamaterials. An important difference of our approach is that instead of transforming the coordinate system (transformation-cloaking optics), we transform instead the medium by allowing our system to be non-Hermitian.

ACKNOWLEDGMENTS

We acknowledge support from the European Commission under project NHQWAVE (Grant No. MSCA-RISE 691209).

[1] N. Moiseyev, *Non-Hermitian Quantum Mechanics* (Cambridge University Press, New York, 2011).
[2] M. V. Berry, Czech. J. Phys. **54**, 1039 (2004).
[3] W. D. Heiss, J. Phys. A **37**, 2455 (2004).
[4] J. Wiersig, S.-W. Kim, and M. Hentschel, Phys. Rev. A **78**, 053809 (2008).
[5] S. B. Lee, J. Yang, S. Moon, S. Y. Lee, J. B. Shim, S. W. Kim, J. H. Lee, and K. An, Phys. Rev. Lett. **103**, 134101 (2009).
[6] C. M. Bender and S. Boettcher, Phys. Rev. Lett. **80**, 5243 (1998).
[7] C. M. Bender, S. Boettcher, and P. N. Meisinger, J. Math. Phys. **40**, 2201 (1999).
[8] C. M. Bender, D. C. Brody, and H. F. Jones, Phys. Rev. Lett. **89**, 270401 (2002).
[9] R. El-Ganainy, K. G. Makris, D. N. Christodoulides, and Z. H. Musslimani, Opt. Lett. **32**, 2632 (2007).
[10] K. G. Makris, R. El-Ganainy, D. N. Christodoulides, and Z. H. Musslimani, Phys. Rev. Lett. **100**, 103904 (2008).
[11] Z. H. Musslimani, K. G. Makris, R. El-Ganainy, and D. N. Christodoulides, Phys. Rev. Lett. **100**, 030402 (2008).
[12] A. Guo, G. J. Salamo, D. Duchesne, R. Morandotti, M. Volatier-Ravat, V. Aimez, G. A. Siviloglou, and D. N. Christodoulides, Phys. Rev. Lett. **103**, 093902 (2009).
[13] C. E. Rüter, K. G. Makris, R. El-Ganainy, D. N. Christodoulides, M. Segev, and D. Kip, Nat. Phys. **6**, 192 (2010).
[14] Y. D. Chong, L. Ge, and A. D. Stone, Phys. Rev. Lett. **106**, 093902 (2011).
[15] L. Ge, Y. D. Chong, and A. D. Stone, Phys. Rev. A **85**, 023802 (2012).
[16] P. Ambichl, K. G. Makris, L. Ge, Y. D. Chong, A. D. Stone, and S. Rotter, Phys. Rev. X **3**, 041030 (2013).
[17] A. Regensburger, C. Bersch, M.-A. Miri, G. Onishchukov, D. N. Christodoulides, and U. Peschel, Nature (London) **488**, 167 (2012).
[18] L. Feng, Y.-L. Xu, W. S. Fegadolli, M.-H. Lu, J. E. B. Oliveira, V. R. Almeida, Y.-F. Chen, and A. Scherer, Nat. Mater. **12**, 108 (2013).
[19] B. Peng, S. K. Ozdemir, F. Lei, F. Monifi, M. Gianfreda, G. L. Long, S. Fan, F. Nori, C. M. Bender, and L. Yang, Nat. Phys. **10**, 394 (2014).
[20] L. Feng, Z. Jing Wong, R.-M. Ma, Y. Wang, and X. Zhang, Science **346**, 972 (2014).
[21] H. Hodaei, M.-A. Miri, M. Heinrich, D. N. Christodoulides, and M. Khajavikhan, Science **346**, 975 (2014).
[22] B. Peng, S. K. Özdemir, S. Rotter, H. Yilmaz, M. Liertzer, F. Monifi, C. M. Bender, F. Nori, and L. Yang, Science **346**, 328 (2014).
[23] S. Assawaworrarit, X. Yu, and S. Fan, Nature (London) **546**, 387 (2017).
[24] J. Zhang, B. Peng, S. K. Özdemir, K. Pichler, D. O. Krimer, G. Zhao, F. Nori, Y. Liu, S. Rotter, and L. Yang, Nat. Photon. **12**, 479 (2018).
[25] T. Kottos, Nat. Phys. **6**, 166 (2010).
[26] V. V. Konotop, J. Yang, and D. A. Zezyulin, Rev. Mod. Phys. **88**, 035002 (2016).
[27] L. Feng, R. El-Ganainy, and L. Ge, Nat. Photon. **11**, 752 (2017).

[28] D. F. Pile and D. N. Christodoulides, Nat. Photon. **11**, 742 (2017).
[29] G. Gbur and K. G. Makris, Photon. Res. **6**, PTS1 (2018).
[30] R. El-Ganainy, K. G. Makris, M. Khajavikhan, Z. H. Musslimani, S. Rotter, and D. N. Christodoulides, Nat. Phys. **14**, 11 (2018).
[31] S. K. Özdemir, S. Rotter, F. Nori, and L. Yang, Nat. Mater. **18**, 783 (2019).
[32] M. A. Miri and A. Alu, Science **363**, eaar7709 (2019).
[33] K. G. Makris, Z. H. Musslimani, D. N. Christodoulides, and S. Rotter, Nat. Commun. **6**, 7257 (2015).
[34] K. G. Makris, Z. H. Musslimani, D. N. Christodoulides, and S. Rotter, IEEE J. Sel. Top. Quantum Electron. **22**, 42 (2016).
[35] J. T. Cole, K. G. Makris, Z. H. Musslimani, D. N. Christodoulides, and S. Rotter, Physica D **336**, 53 (2016).
[36] K. G. Makris, A. Brandstötter, P. Ambichl, Z. H. Musslimani, and S. Rotter, Light Sci. Appl. **6**, e17035 (2017).
[37] E. Rivet, A. Brandstötter, K. G. Makris, H. Lissek, S. Rotter, and R. Fleury, Nat. Phys. **14**, 942 (2018).
[38] S. Yu, X. Piao, and N. Park, Phys. Rev. Lett. **120**, 193902 (2018).
[39] A. Brandstötter, K. G. Makris, and S. Rotter, Phys. Rev. B **99**, 115402 (2019).
[40] K. G. Makris, I. Kresic, A. Brandstötter, and S. Rotter, Optica **7**, 619 (2020).
[41] I. M. Vellekoop, A. Lagendijk, and A. P. Mosk, Nat. Photon. **4**, 320 (2010).
[42] O. Katz, E. Small, Y. Bromberg, and Y. Silberberg, Nat. Photon. **5**, 372 (2011).
[43] N. Bachelard, S. Gigan, X. Noblin, and P. Sebbah, Nat. Phys. **10**, 426 (2014).
[44] T. Hisch, M. Liertzer, D. Pogany, F. Mintert, and S. Rotter, Phys. Rev. Lett. **111**, 023902 (2013).
[45] S. Rotter and S. Gigan, Rev. Mod. Phys. **89**, 015005 (2017).
[46] S. Suntsov, K. G. Makris, D. N. Christodoulides, G. I. Stegeman, R. Morandotti, M. Volatier, V. Aimez, R. Arès, C. E. Rüter, and D. Kip, Opt. Express **15**, 4663 (2007).
[47] S. Suntsov, K. G. Makris, D. N. Christodoulides, G. I. Stegeman, R. Morandotti, M Volatier, V. Aimez, R. Ares, E. H. Yang, and G. Salamo, Opt. Express **16**, 10480 (2008).
[48] M. J. Ablowitz and Z. H. Musslimani, Opt. Lett. **30**, 2140 (2005).
[49] M. J. Ablowitz and Z. H. Musslimani, Physica D **184**, 276 (2003).
[50] M. Wadati, J. Phys. Soc. Jpn. **77**, 074005 (2008).
[51] J. K. Yang, Opt. Lett. **39**, 5547 (2014).
[52] V. V. Konotop, and D. A. Zezyulin, Opt. Lett. **39**, 5535 (2014).
[53] D. A. Zezyulin, I. V. Barashenkov, and V. V. Konotop, Phys. Rev. A **94**, 063649 (2016).
[54] I. V. Barashenkov, D. A. Zezyulin, and V. V. Konotop, in *Selected Contributions from the 15th International Conference on Non-Hermitian Hamiltonians in Quantum Physics, Palermo, Italy, 2015*, edited by F. Bagarello, R. Passante, and C. Trapani, Springer Proceedings in Physics No. 184 (Springer International, Switzerland, 2016), p. 143.
[55] G. Kaniadakis and A. M. Scarfone, J. Phys. A **35**, 1943 (2002).
[56] F. Correa, V. Jakubsky, and M. S. Plyushchay, Phys. Rev. A **92**, 023839 (2015).
[57] M. J. Ablowitz and Z. H. Musslimani, Phys. Rev. Lett. **110**, 064105 (2013).